

Leptogenesis with Single Right-Handed Neutrino Dominance

M. Hirsch and S. F. King

*Department of Physics and Astronomy, University of Southampton,
Southampton, SO17 1BJ, U.K.*

Abstract

We make an analytic and numerical study of leptogenesis in the framework of the (Supersymmetric) Standard Model plus the see-saw mechanism with a $U(1)$ family symmetry and single right-handed neutrino dominance. In presenting our analytic and numerical results we make a clear distinction between the theoretically clean asymmetry parameter ϵ_1 and the baryon asymmetry Y_B . In calculating Y_B we propose and use a fit to the solutions to the Boltzmann equations which gives substantially more reliable results than parametrisations previously used in the literature. Our results show that there is a decoupling between the low energy neutrino observables and the leptogenesis predictions, but that nevertheless leptogenesis is capable of resolving ambiguities within classes of models which would otherwise lead to similar neutrino observables. For example we show that models where the dominant right-handed neutrino is the heaviest are preferred to models where it is the lightest and study an explicit example of a unified model of this type.

1 Introduction

Leptogenesis is an interesting mechanism which has been proposed to generate the observed baryon asymmetry of the Universe (BAU) [1, 2]. The mechanism involves the out-of-equilibrium decay of a heavy right handed neutrino N_R . The net lepton number L produced in the decay is then re-processed into baryon number B by anomalous (B+L) violating sphaleron interactions, which otherwise conserve (B-L) [3].

The advantage of this mechanism is that the same physics that allows the right handed neutrinos to decay into light leptons is also responsible for a see-saw neutrino mass matrix [4]. This point of view has been strengthened by the latest experimental data on the solar neutrino problem by SNO [5] and Super-Kamiokande [6] which, when combined, now seems to confirm the existence of a solar neutrino mass scale, and suggests active neutrino oscillations based on either the LMA or the LOW solution [7]. This in turn gives impetus to the see-saw mechanism. Combining the see-saw mechanism with the experimental data [5, 6] seems to favour scales for right handed neutrino masses M_R in the range $10^7 - 10^{16}$ GeV. There have been many studies of leptogenesis, all based on different models, for example left-right symmetry, SO(10), and so on [8].

In this paper we study leptogenesis in the framework of the (Supersymmetric) Standard Model plus the see-saw mechanism with single right-handed neutrino dominance [9], [10]. SRHND is useful for both the LMA and the LOW solution [10] since it leads to a natural neutrino mass hierarchy in the presence of large mixing angles, and gives results which are stable under radiative corrections [11]. This provides a relatively model independent approach which applies to a large class of models with a natural hierarchy of neutrino masses [12]. Indeed in the case of the LOW solution, SRHND is almost inevitable in order to maintain the large neutrino mass hierarchy present in this case.

Within the SRHND framework we generalise previously presented analytic estimates for the mixing angles to the complex domain, and present new analytic results for the leptogenesis asymmetry parameter ϵ_1 and discuss the insights which this leads to. We then introduce a $U(1)$ family symmetry [13] and discuss our numerical approach to models of this kind. Our analytic results above are supported by the detailed numerical analysis of various texture models. Texture models involve unknown coefficients mul-

tipling the expansion parameters, which implies some level of uncertainty in the predictions. In order to quantify this we perform a numerical scan over the unknown coefficients, to obtain distributions for predictions of neutrino masses, mixing angles as well as the predictions for ϵ_1 and the baryon asymmetry Y_B , for different classes of models. In presenting our analytic and numerical results we make a clear distinction between the theoretically clean asymmetry parameter ϵ_1 and the baryon asymmetry Y_B . In calculating Y_B we propose and use a fit to the solutions to the Boltzmann equations which gives substantially more reliable results than parametrisations previously used in the literature. Using the numerical approach, supported by the analytic estimates, we then discuss two important aspects of leptogenesis, namely leptogenesis decoupling and leptogenesis discrimination.

We demonstrate explicitly that there is a *decoupling* between leptogenesis and the experimentally measurable neutrino parameters. Although such a result may be inferred by comparing the results from different individual models which have been proposed in the literature, the present paper represents the first attempt to systematically demonstrate this within a framework (SRHND) which can be plausibly applied to many different models. To support the decoupling claim we present examples of classes of models which give the same measurable neutrino parameters but have very different values for the CP asymmetry ϵ_1 . Leptogenesis decoupling implies that there is no relation for example between the size of the solar neutrino angle or MNS phase and the baryon asymmetry predicted by leptogenesis.

On the other hand we show that leptogenesis is capable of *discriminating* between different models and thereby resolving ambiguities within classes of models giving the same low energy predictions. For example leptogenesis may resolve the ambiguity as to whether the dominant right-handed neutrino (the one chiefly responsible for the atmospheric neutrino mass in hierarchical models) is the heaviest or the lightest of the right-handed neutrinos. We show that within a standard hot big bang universe the models where the dominant right-handed neutrino is the heaviest are preferred and are more consistent with the gravitino constraint on the reheat temperature $T_R \lesssim 10^9 \text{GeV}$ [15].

In section 2 we introduce our conventions, especially the use of the diagonal charged lepton and right-handed neutrino basis, the see-saw mechanism and the MNS matrix in this basis, and the standard model leptogenesis formulae in this basis. In calculating the baryon asymmetry Y_B in section 2.3 we present and use a new fit formula based on a Boltzmann analysis. In

section 3 we give our analytic results based on SRHND for the MNS parameters and leptogenesis, which give important insights into the numerical results which follow. In section 4 we discuss our numerical approach to $U(1)$ family symmetry models. Section 5 is a discussion of the decoupling feature of leptogenesis based on the calculation of the asymmetry parameter ϵ_1 . In section 6 we discuss the calculation of Y_B for the models where the dominant right-handed neutrino is the lightest, and show that such models are not consistent with a standard hot big bang scenario. In section 7 we then discuss models where the dominant right-handed neutrino is the heaviest and show that such models can lead to successful leptogenesis. Section 8 concludes the paper.

2 Conventions

2.1 The Diagonal Charged Lepton and Right-Handed Neutrino Basis

To fix the notation we consider the Yukawa terms with two Higgs doublets augmented by 3 right-handed neutrinos, which, ignoring the quarks, are given by

$$\mathcal{L}_{yuk} = \epsilon_{ab} \left[\tilde{Y}_{ij}^e H_d^a L_i^b E_j^c - \tilde{Y}_{ij}^\nu H_u^a L_i^b N_j^c + \frac{1}{2} \tilde{Y}_{RR}^{ij} \Sigma N_i^c N_j^c \right] + H.c. \quad (1)$$

where $\epsilon_{ab} = -\epsilon_{ba}$, $\epsilon_{12} = 1$, and the remaining notation is standard except that the 3 right-handed neutrinos N_R^p have been replaced by their CP conjugates N_i^c and we have introduced a singlet field Σ whose vacuum expectation value (VEV) induces a heavy complex symmetric Majorana matrix $\tilde{M}_{RR} = \langle \Sigma \rangle \tilde{Y}_{RR}$. When the two Higgs doublets get their VEVs $\langle H_u^2 \rangle = v_2$, $\langle H_d^1 \rangle = v_1$ we find the terms ¹

$$\mathcal{L}_{yuk} = v_1 \tilde{Y}_{ij}^e E_i E_j^c + v_2 \tilde{Y}_{ij}^\nu N_i N_j^c + \frac{1}{2} \tilde{M}_{RR}^{ij} N_i^c N_j^c + H.c. \quad (2)$$

Replacing CP conjugate fields we can write in a matrix notation

$$\mathcal{L}_{yuk} = \bar{E}_L v_1 \tilde{Y}^{e*} E_R + \bar{N}_L v_2 \tilde{Y}^{\nu*} N_R + \frac{1}{2} N_R^T \tilde{M}_{RR}^* N_R + H.c. \quad (3)$$

¹In the case of the standard model we must replace one of the two Higgs doublets by the charge conjugate of the other, $H_d = H_u^c$.

It is convenient to work in the diagonal charged lepton basis

$$\text{diag}(m_e, m_\mu, m_\tau) = V_{eL} v_1 \tilde{Y}^e{}^* V_{eR}^\dagger \quad (4)$$

and the diagonal right-handed neutrino basis

$$\text{diag}(M_1, M_2, M_3) = V_{\nu R} \tilde{M}^*{}_{RR} V_{\nu R}^T \quad (5)$$

where $V_{eL}, V_{eR}, V_{\nu R}$ are unitary transformations. In this basis the neutrino Yukawa couplings are given by

$$Y^\nu = V_{eL} \tilde{Y}^{\nu*} V_{\nu R}^T \quad (6)$$

and the Lagrangian in this basis is

$$\begin{aligned} \mathcal{L}_{yuk} &= (\bar{e}_L \bar{\mu}_L \bar{\tau}_L) \text{diag}(m_e, m_\mu, m_\tau) (e_R \mu_R \tau_R)^T \\ &+ (\bar{\nu}_{eL} \bar{\nu}_{\mu L} \bar{\nu}_{\tau L}) Y^\nu v_2 (N_{R1} N_{R2} N_{R3})^T \\ &+ (N_{R1} N_{R2} N_{R3}) \text{diag}(M_1, M_2, M_3) (N_{R1} N_{R2} N_{R3})^T + H.c. \end{aligned} \quad (7)$$

2.2 The See-Saw Mechanism and the MNS Matrix in this Basis

The light effective left-handed Majorana neutrino mass matrix in the above basis is

$$m_{LL} = v_2^2 Y^\nu \text{diag}(M_1^{-1}, M_2^{-1}, M_3^{-1}) Y^{\nu T} \quad (8)$$

Having constructed the complex symmetric light Majorana mass matrix it must then be diagonalised by,

$$V_{\nu L} m_{LL} V_{\nu L}^T = \text{diag}(|m_1|, |m_2|, |m_3|) \quad (9)$$

where $V_{\nu L}$ is a unitary transformation and the neutrino mass eigenvalues are real and positive. The leptonic analogue of the CKM matrix is the MNS matrix defined as [14]

$$U_{MNS} = V_{eL} V_{\nu L}^\dagger, \quad (10)$$

where in the diagonal charged lepton basis V_{eL} will only consist of a diagonal matrix of phases, $V_{eL} = P_e$ corresponding to the charged lepton phase freedom,

$$\begin{pmatrix} e \\ \mu \\ \tau \end{pmatrix}_{L,R} \rightarrow P_e \begin{pmatrix} e \\ \mu \\ \tau \end{pmatrix}_{L,R} \quad (11)$$

where

$$P_e = \begin{pmatrix} e^{i\phi_1} & 0 & 0 \\ 0 & e^{i\phi_2} & 0 \\ 0 & 0 & e^{i\phi_3} \end{pmatrix} \quad (12)$$

These transformations leave the charged lepton masses real and positive, and enable three phases to be removed from the unitary matrix $V_{\nu L}$, so that U_{MNS} can be parameterized in terms of three mixing angles θ_{ij} and three complex phases δ_{ij} , by regarding it as a product of three complex Euler rotations,

$$U_{MNS} = U_{23}U_{13}U_{12} \quad (13)$$

where

$$U_{23} = \begin{pmatrix} 1 & 0 & 0 \\ 0 & c_{23} & s_{23}e^{-i\delta_{23}} \\ 0 & -s_{23}e^{i\delta_{23}} & c_{23} \end{pmatrix} \quad (14)$$

$$U_{13} = \begin{pmatrix} c_{13} & 0 & s_{13}e^{-i\delta_{13}} \\ 0 & 1 & 0 \\ -s_{13}e^{i\delta_{13}} & 0 & c_{13} \end{pmatrix} \quad (15)$$

$$U_{12} = \begin{pmatrix} c_{12} & s_{12}e^{-i\delta_{12}} & 0 \\ -s_{12}e^{i\delta_{12}} & c_{12} & 0 \\ 0 & 0 & 1 \end{pmatrix} \quad (16)$$

where $c_{ij} = \cos \theta_{ij}$ and $s_{ij} = \sin \theta_{ij}$. The resulting MNS matrix is:

$$\begin{pmatrix} c_{12}c_{13} & s_{12}c_{13}e^{-i\delta_{12}} & s_{13}e^{-i\delta_{13}} \\ -s_{12}c_{23}e^{i\delta_{12}} - c_{12}s_{23}s_{13}e^{i(\delta_{13}-\delta_{23})} & c_{12}c_{23} - s_{12}s_{23}s_{13}e^{i(-\delta_{23}+\delta_{13}-\delta_{12})} & s_{23}c_{13}e^{-i\delta_{23}} \\ s_{12}s_{23}e^{i(\delta_{23}+\delta_{12})} - c_{12}c_{23}s_{13}e^{i\delta_{13}} & -c_{12}s_{23}e^{i\delta_{23}} - s_{12}c_{23}s_{13}e^{i(\delta_{13}-\delta_{12})} & c_{23}c_{13} \end{pmatrix} \quad (17)$$

The Dirac phase which enters the CP odd part of neutrino oscillation probabilities is given by

$$\delta = \delta_{13} - \delta_{23} - \delta_{12}. \quad (18)$$

2.3 Leptogenesis in this Basis

CP violation in the decay of the lightest right-handed neutrino N_{R1} comes from the interference between the tree-level and one-loop amplitudes [2, 8,

16, 17]. The CP asymmetries given by the interference with the one-loop vertex amplitude are in the SM [2, 8]:

$$\begin{aligned}\epsilon_1 &= \frac{\Gamma(N_{R1} \rightarrow L_j + H_2) - \Gamma(N_{R1}^\dagger \rightarrow L_j^\dagger + H_2^\dagger)}{\Gamma(N_{R1} \rightarrow L_j + H_2) + \Gamma(N_{R1}^\dagger \rightarrow L_j^\dagger + H_2^\dagger)} \\ &= \frac{1}{8\pi(Y_\nu^\dagger Y_\nu)_{11}} \sum_{i \neq 1} \text{Im} \left([(Y_\nu^\dagger Y_\nu)_{1i}]^2 \right) \left(f\left(\frac{M_1^2}{M_i^2}\right) + g\left(\frac{M_1^2}{M_i^2}\right) \right)\end{aligned}\quad (19)$$

where

$$f(x) = \sqrt{x} \left[1 - (1+x) \ln \left(\frac{1+x}{x} \right) \right], \quad g(x) = \frac{\sqrt{x}}{1-x}, \quad (20)$$

where $f(x)$ arises from the interference between the tree level decay and the vertex correction, while $g(x)$ is due to the interference with the absorptive part of the one-loop self-energy, which can in principle be much larger if the right-handed neutrinos are almost degenerate [16, 17]. Assuming that $M_1 \ll M_2 \ll M_3$, we have approximately [18],

$$\epsilon_1 \approx -\frac{3}{16\pi(Y_\nu^\dagger Y_\nu)_{11}} \sum_{i \neq 1} \text{Im} \left([(Y_\nu^\dagger Y_\nu)_{1i}]^2 \right) \left(\frac{M_1}{M_i} \right) \quad (21)$$

In the Supersymmetric SM the result for ϵ_1 is twice as large as in Eq.21 due to the extra SUSY degrees of freedom in the diagrams.

The lepton asymmetry Y_L of the universe created by this mechanism can be written as

$$Y_L = d \frac{\epsilon_1}{g^*} \quad (22)$$

where ϵ_1 has been defined above, g^* counts the effective number of degrees of freedom, for the SM $g^* = 106.75$ while for the Supersymmetric SM $g^* = 228.75$ [20] and d is the dilution factor which takes into account the washout effect produced by inverse decay and lepton number violating scattering. To calculate d one has to solve, in principle, the full Boltzman equations, which can be done numerically [2, 18].

However, many authors, for examples see [20], have used simple approximated solutions to the Boltzman equations expressed as [20]

$$d = \frac{0.24}{k(\ln k)^{3/5}} \quad 10 \leq k \leq 10^6 \quad (23)$$

$$d = \frac{1}{2k} \quad 1 \leq k \leq 10 \quad (24)$$

$$d = 1 \quad 0 \leq k \leq 1 \quad (25)$$

Recently, Nielson and Takanishi [21] suggested a slight modification of eqs (23)-(25), namely,

$$d = \frac{0.3}{k(\ln k)^{3/5}} \quad 10 \leq k \leq 10^6 \quad (26)$$

$$d = \frac{1}{2\sqrt{k^2 + 9}} \quad k \leq 10 \quad (27)$$

Here the parameter k is given by,

$$k = \frac{M_P}{1.7 \times 8\pi\sqrt{g^*}} \frac{(Y_\nu^\dagger Y_\nu)_{11}}{M_1} \quad (28)$$

where M_P is the Planck mass. Physically $k \sim 1$ represents the desirable region where the couplings of the right-handed neutrinos are sufficiently strong for them to be copiously produced from particles in the thermal bath, but sufficiently weak for them to decay satisfying the out-of-equilibrium condition.

We have compared eqs (26)-(27) to the full numerical solution to the Boltzman equations as plotted in fig. 6 of [19]. Buchmüller and Plümacher [19] use as a variable

$$\tilde{m}_1 = v^2 \frac{(Y_\nu^\dagger Y_\nu)_{11}}{M_1} \simeq 1.1 \times 10^{-3} k \text{ eV}. \quad (29)$$

The result of this comparison is shown in Fig. 1. As one can see, the approximate formulas, eqs (26)-(27), are a valid approximation for values of $k \sim 1$ and for small values of $M_1 \leq 10^{10}$ GeV. For smaller values of $k \ll 1$ or $\tilde{m}_1 \ll 10^{-3}$ eV the approximation formulas are clearly not valid since they do not take into account the production suppression apparent in the full treatment using the Boltzmann equations. For larger values of $k \gg 1$ or $\tilde{m}_1 \gg 10^{-3}$ eV (and larger values of M_1) the approximation formulas are also clearly not valid since they do not take into account the steep suppression due to the out-of-equilibrium condition being violated which is again apparent in the full treatment using the Boltzmann equations. From Fig. 1 it is obvious

that in this case the analytic approximation seriously underestimates the suppression of d by orders of magnitude.

For this reason we have devised a purely empirical fit formula for the exact solution to the Boltzman equations, which can be written as,

$$(a) \text{ Log}_{10}(d_{B-L}) = 0.8 * \text{Log}_{10}(\tilde{m}_1) + 1.7 + 0.05 * \text{Log}_{10}(M_1^{10}) \quad (30)$$

$$(b) \text{ Log}_{10}(d_{B-L}) = -1.2 - 0.05 * \text{Log}_{10}(M_1^{10}) \quad (31)$$

$$(c) \text{ Log}_{10}(d_{B-L}) = -(3.8 + \text{Log}_{10}(M_1^{10})) * (\text{Log}_{10}(\tilde{m}_1) + 2) \quad (32)$$

$$- (5.4 - \frac{2}{3} * \text{Log}_{10}(M_1)) ^2 - \frac{3}{2}$$

where $M_1^{10} = M_1/10^{10}\text{GeV}$, \tilde{m}_1 is in units of [eV]. In implementing this fit it is always the smallest of (a)-(c) which is taken. ² The results of this fit are superimposed onto the exact curves taken from [19] in Fig. 1.

Obviously eqs. (30)- (32) reproduce the exact results considerably better than eqs (26)-(27). However, in [19] the authors assumed that right-handed neutrinos are hierarchical. Also we have to assume that for small values of ϵ_1 the dilution function does not depend on ϵ_1 . Thus, eqs (30)- (32) are still approximate, and may not be valid if these conditions are violated. Moreover, for large values of M_1 , say $M_1 \sim 10^{14}$, we have to rely on an extrapolation beyond values of M_1 used in the fit.

Note also that since in the SUSY SM both ϵ_1 and g^* are twice as large as in the SM, the two effects tend to cancel in the estimate of Y_L . Also the approximations for d over the above range of \tilde{m}_1 are valid for either the SM or the SUSY SM [20]. Therefore the results we present are approximately valid for either the SM or the SUSY SM, although for definiteness we consider the SM from now on.

Due to sphaleron effects Y_L finally is related to Y_B approximately via [22]

$$Y_B = \frac{\alpha}{\alpha - 1} Y_L \quad (33)$$

where

$$\alpha = \frac{8N_F + 4N_H}{22N_F + 13N_H} \quad (34)$$

²We fit d_{B-L} since authors of [19] plot Y_{B-L} , where d_{B-L} is related to d via $d = (1 - \alpha)d_{B-L}$, where α is defined in Eq.34.

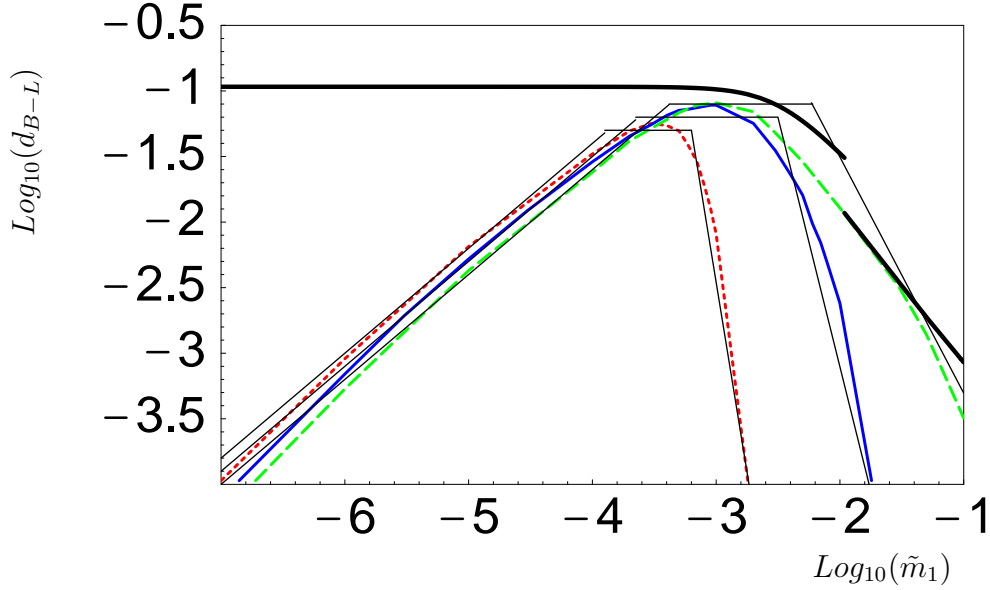


Figure 1: The logarithm of the dilution function d_{B-L} versus the logarithm of \tilde{m}_1 for different values of the lightest right-handed neutrino mass $M_1 = 10^8, 10^{10}, 10^{12}$ GeV (from right to left). The thick line is the solution to Eqs.(26)-(27). The dashed, medium full, dotted curves represent d_{B-L} for $M_1 = 10^8, 10^{10}, 10^{12}$ GeV extracted from Fig.(6) of [19], based on an exact numerical solution of the Boltzman equation. The thin solid curves with plateau regions are the approximately fitted values of d_{B-L} following Eqs. (30)-(32).

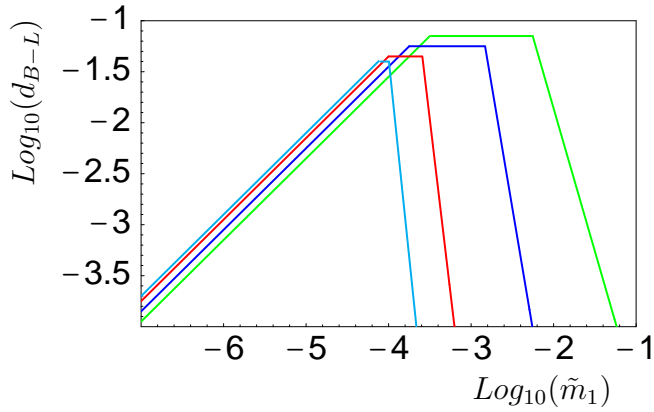


Figure 2: The approximate solutions of the fit function for d_{B-L} from Eqs.(30)-(32) for (from right to left) $M_1 = 10^9, 10^{11}, 10^{13}, 10^{14}$ GeV. For further discussion see caption in Fig.1.

Here N_F is the number of families and N_H the number of Higgs doublets. In the SM $\alpha \simeq 1/3$. Experimentally Y_B is expected to be in the range $Y_B = (n_B - n_{\bar{B}})/s \sim (0.5 - 1) \times 10^{-10}$ [8, 17].

3 Analytic Estimates

3.1 MNS Parameters from SRHND

In the basis used in this paper where the charged leptons are diagonal, and the right-handed neutrinos are diagonal, we write the neutrino Yukawa matrix as

$$Y_\nu = \begin{pmatrix} a' & a & d \\ b' & b & e \\ c' & c & f \end{pmatrix} \quad (35)$$

where the LR notation means that the second and third columns of Y_ν correspond to the second and third right-handed neutrinos. We use the phase freedom of the charged lepton masses in Eq.11 to make the couplings to the third right-handed neutrino d, e, f real and positive, leaving a, b, c, a', b', c' complex.

We write the diagonal (real, positive) Majorana masses in this basis as

$$M_{RR} = \begin{pmatrix} X' & 0 & 0 \\ 0 & X & 0 \\ 0 & 0 & Y \end{pmatrix} \quad (36)$$

Then using the see-saw formula for the light effective Majorana mass matrix $m_{LL} = v_2^2 Y_\nu M_{RR}^{-1} Y_\nu^T$ (valid for complex couplings) we find the symmetric matrix,

$$m_{LL} = \begin{pmatrix} \frac{a'^2}{X'} + \frac{a^2}{X} + \frac{d^2}{Y} & \frac{a'b'}{X'} + \frac{ab}{X} + \frac{de}{Y} & \frac{a'c'}{X'} + \frac{ac}{X} + \frac{df}{Y} \\ \cdot & \frac{b'^2}{X'} + \frac{b^2}{X} + \frac{e^2}{Y} & \frac{b'c'}{X'} + \frac{bc}{X} + \frac{ef}{Y} \\ \cdot & \cdot & \frac{c'^2}{X'} + \frac{c^2}{X} + \frac{f^2}{Y} \end{pmatrix} \quad (37)$$

So far the discussion is completely general. In order to account for the atmospheric and solar neutrino data many models have been proposed [12] based on the see-saw mechanism [4]. One question which is common to all these models is how to arrange for a large mixing angle involving the second

and third generation of neutrinos, without destroying the hierarchy of mass splittings necessary to account for the solar and atmospheric data. Assuming $\theta_{23} \sim \pi/4$ one might expect two similar eigenvalues $m_2 \sim m_3$, and then a hierarchy of neutrino masses seems rather unnatural.

For our analytic estimates, we assume for simplicity that the first right-handed neutrino X' contributions are insignificant compared to the second right-handed neutrino X contributions,

$$\frac{|a' + b' + c'|^2}{X'} \ll \frac{|a + b + c|^2}{X} \quad (38)$$

Then one way to achieve a natural hierarchy is to suppose that the third right-handed neutrino contributions are much greater than the second right-handed neutrino contributions in the 23 block of m_{LL} [10],

$$\frac{(e^2, ef, f^2)}{Y} \gg \frac{|a + b + c|^2}{X} \quad (39)$$

This implies an approximately vanishing 23 subdeterminant,

$$\det[m_{LL}]_{23} = \left(\frac{e^2}{Y} + \frac{b^2}{X}\right) \left(\frac{f^2}{Y} + \frac{c^2}{X}\right) - \left(\frac{ef}{Y} + \frac{bc}{X}\right)^2 \approx 0 \quad (40)$$

and hence

$$m_2/m_3 \ll 1 \quad (41)$$

Thus the assumption in Eq.39 that the right-handed neutrino Y gives the dominant contribution to the 23 block of m_{LL} naturally leads to a neutrino mass hierarchy. This mechanism is called single right-handed neutrino dominance (SRHND)[9]. In the limit that only a single right handed neutrino contributes the determinant clearly exactly vanishes and we have $m_2 = 0$ exactly. However the sub-dominant contributions from the right-handed neutrino X will give a small finite mass $m_2 \neq 0$ as required by the MSW solution to the solar neutrino problem.

Assuming SRHND as discussed above, we may obtain a simple estimate for the third neutrino mass:

$$m_3 \approx v_2^2 \frac{(d^2 + e^2 + f^2)}{Y} \quad (42)$$

Note that $m_{1,2}$ are determined by parameters associated with the subdominant right-handed neutrinos and so are naturally smaller. Given the SRHND assumption in Eq.39 we see that we have generated a hierarchical spectrum $|m_{1,2}| \ll |m_3|$.

In order to obtain the MNS parameters we must diagonalise m_{LL} as in Eq.9,

$$V_{\nu L} m_{LL} V_{\nu L}^T = \text{diag}(|m_1|, |m_2|, |m_3|) \quad (43)$$

where we write $V_{\nu L}$ as a product of complex Euler rotations of the form of Eqs.13,14,15,16, together with diagonal phase matrix

$$P_\nu = \begin{pmatrix} e^{i\tilde{\phi}_1/2} & 0 & 0 \\ 0 & e^{i\tilde{\phi}_2/2} & 0 \\ 0 & 0 & e^{i\tilde{\phi}_3/2} \end{pmatrix} \quad (44)$$

which is required to remove the phases in $m_i = |m_i|e^{i\tilde{\phi}_i}$,

$$V_{\nu L} = P_\nu^\dagger \tilde{U}_{12}^\dagger \tilde{U}_{13}^\dagger \tilde{U}_{23}^\dagger \quad (45)$$

Thus $V_{\nu L}$ contains the 3 angles and 6 phases of a general unitary matrix. However in the basis where we have chosen the couplings d, e, f to be real, m_3 is given in Eq.42 and $\tilde{\phi}_3$ is zero to leading order.

In order to bring the MNS matrix into the form in Eq.17, additional charged lepton phase rotations are required as in Eqs.10, so that we have finally

$$U_{MNS} = P_e \tilde{U}_{23} \tilde{U}_{13} \tilde{U}_{12} P_\nu \quad (46)$$

where P_e is a diagonal matrix of phases as in Eq.12. Note that the angles involved in the \tilde{U}_{ij} are the same as those in the U_{ij} in Eq.13, $\tilde{\theta}_{ij} = \theta_{ij}$, but the phases will be different, $\tilde{\delta}_{ij} \neq \delta_{ij}$, due to the non-zero phases in P_e, P_ν .

Since the couplings d, e, f are real, we find that the previous estimates based on SRHND are still valid [10]

$$\tan \theta_{23} \approx \frac{e}{f}, \quad (47)$$

$$\tan \theta_{13} \approx \frac{d}{\sqrt{e^2 + f^2}} \quad (48)$$

where the associated phases are approximately zero

$$\tilde{\delta}_{23} \approx \tilde{\delta}_{13} \approx 0 \quad (49)$$

By a suitable choice of parameters $e = f \gg d$ it is possible to have maximal θ_{23} suitable for atmospheric oscillations, while maintaining a small θ_{13} consistent with the CHOOZ constraint [23].

To determine U_{12} is quite complicated in general, but in the physically interesting cases where θ_{12} is near maximal $\theta_{12} \approx \pi/4$ we find the simple analytical results

$$\tan \theta_{12} \approx \sqrt{2} \frac{|a|}{|b-c|} \quad (50)$$

$$\tilde{\delta}_{12} \approx \phi_{b-c} - \phi_a \quad (51)$$

where $\phi_{b-c} = \arg(b-c)$ and $\phi_a = \arg(a)$. In the simple example that the phases in P_e, P_ν are zero, the observable Dirac phase in Eq.18 is given in Eq.51. In general the Dirac phase will involve a more complicated combination of phases.

3.2 Leptogenesis in SRHND

In leptogenesis it is generally the lightest right-handed neutrino which decays to produce lepton number, where we use the notation that M_1 is the lightest right-handed neutrino, M_3 is the heaviest right-handed neutrino and we assume $M_1 \ll M_2 \ll M_3$. In the notation of the previous subsection where Y is the dominant right-handed neutrino there are two physically distinct cases to consider:

- (a) $Y \ll X \ll X'$ (i.e. $Y = M_1, X = M_2, X' = M_3$)
- (b) $X' \ll X \ll Y$ (i.e. $X' = M_1, X = M_2, Y = M_3$)

In other words the dominant right-handed neutrino may either be (a) the lightest, or (b) the heaviest right-handed neutrino, and both cases must be considered.

It is also worth emphasising that there is no generation ordering implied by the results in the previous subsection (or those in [9],[10]). In other words the dominant right-handed neutrino Y may be associated with the third, second or first generation, by a simple reordering of the columns of Y_ν . Due to the hierarchy of charged lepton masses, it is meaningful to associate the

first row of Y_ν with the first generation, the second row of Y_ν with the second generation, and the third row of Y_ν with the third generation. However the physical neutrino mass matrix m_{LL} is invariant under the operation of exchanging the *columns* of Y_ν , along with the ordering of the right-handed neutrinos in M_{RR} , so the SRHND results apply quite generally to all generation orderings of the right-handed neutrinos [9], [10]. Physically if the Yukawa couplings e, f are of order unity, then it may be natural to associate Y with the third generation. However if the couplings $e, f \ll 1$ then it may be more natural to associate Y with the second generation, and re-order the matrices by interchanging of the second and third right-handed neutrinos in Y_ν and M_{RR} .

Returning to the leptogenesis asymmetry parameter in Eq.21, for case (a), where the dominant right-handed neutrino mass Y is the lightest, using the SRHND results of the previous subsection, we find

$$\epsilon_1^{(a)} \approx -\frac{3}{32\pi} \left(\frac{Y}{X}\right) \sin(2\phi_{b+c})|b+c|^2 \quad (52)$$

while for case (b), where the dominant right-handed neutrino mass Y is the heaviest, we find

$$\epsilon_1^{(b)} \approx \frac{3}{16\pi} \left(\frac{X'}{Y}\right) \sin(2\phi_{b'+c'})e^2 \frac{|b'+c'|^2}{|a'|^2 + |b'|^2 + |c'|^2} \quad (53)$$

where $\phi_{b+c} = \arg(b+c)$ and $\phi_{b'+c'} = \arg(b'+c')$, and we have used the fact that $m_2 \ll m_3$ in obtaining Eq.53.³

Are these values of ϵ_1 of the correct order of magnitude? We may use $m_3 \sim 5 \times 10^{-2} \text{eV}$ and $m_3 \approx v_2^2 \frac{(2e^2)}{Y}$ in Eq.42, and the crude order of magnitude approximation for $m_2 \sim |b-c|^2 v_2^2 / M_2$, to obtain

$$\epsilon_1^{(a)} \sim \sin(2\phi_{b+c}) 10^{-5} \left(\frac{m_2}{m_3}\right) \left(\frac{Y}{10^{11} \text{GeV}}\right) \quad (54)$$

$$\epsilon_1^{(b)} \sim \sin(2\phi_{b'+c'}) 10^{-6} \left(\frac{X'}{10^{10} \text{GeV}}\right) \quad (55)$$

³It is also apparent that the phases which are relevant for leptogenesis in both cases are not identical to the Dirac phase which even in the simple example that the phases in P_e, P_ν are zero, is given as in Eq.18 as $\delta \approx \phi_a - \phi_{b-c}$. In general the Dirac phase will involve a more complicated combination of phases still.

The results in Eqs.54, 55 express ϵ_1 in terms of the lightest right-handed neutrino mass in each case. Since $\epsilon_1^{(a)}$ is suppressed relative to $\epsilon_1^{(b)}$ by a factor of m_2/m_3 (which should be $m_2/m_3 < 0.1$), this implies that the lightest right-handed neutrino mass must be at least an order of magnitude larger in case (a) than in case (b).⁴

To understand which of the two cases (a) or (b) is more promising from the point of view of leptogenesis it is important to estimate the parameter \tilde{m}_1 in Eq.29 which controls the dilution factor as shown in Figs. 1,2. From Eqs.29,35,

$$\tilde{m}_1^{(a)} \simeq v_2^2 \frac{(|d|^2 + |e|^2 + |f|^2)}{Y} \quad (56)$$

$$\tilde{m}_1^{(b)} \simeq v_2^2 \frac{(|a'|^2 + |b'|^2 + |c'|^2)}{X'} \quad (57)$$

In case (a), where the dominant right-handed neutrino is the lightest one, the parameter $\tilde{m}_1^{(a)}$ in Eq.56 is approximately equal to the physical mass of the heaviest neutrino in Eq.42 which is measured by Super-Kamiokande. Thus for these models $\tilde{m}_1^{(a)} \sim m_3 \sim 5 \times 10^{-2}$ eV which is generally beyond the plateau regions in Figs.1, 2, and this leads to the requirement that $Y \sim M_1 < 10^9$ GeV and a strong dilution suppression $d \ll 1$. However, according to Eq.54, $Y \sim M_1 < 10^9$ GeV leads to values of $\epsilon_1^{(a)} < 10^{-8}$ which, when combined with the dilution suppression $d \ll 1$, implies from Eq.22 $Y_B \ll 10^{-10}$ well below the observed value.

In case (b), on the other hand, where the dominant right-handed neutrino is the heaviest one, there is no association of $\tilde{m}_1^{(b)}$ in Eq.57 with a physical neutrino mass and so this parameter may in principle take smaller values closer to the plateau regions, leading to only a mild dilution suppression $d \lesssim 0.1$ for a range of lightest right-handed neutrino mass X' . Furthermore, as we already remarked, by comparing Eqs.54, 55 we see that value of $\epsilon_1^{(b)}$ is larger by an order of magnitude than $\epsilon_1^{(a)}$. For example if we choose $X' \sim M_1 \lesssim 10^9$ GeV, consistent with the gravitino constraint on the reheating temperature $T_R \lesssim 10^9$ GeV [15], we find $\epsilon_1^{(b)} \lesssim 10^{-7}$ which, assuming a mild

⁴Note that since the dominant right-handed neutrino mass is given by $Y \sim e^{25.10^{14}}$ GeV, case (a) requires $e \ll 1$, whereas for case (b) it is consistent with $e \sim 1$ providing there is a sufficiently large hierarchy in the right-handed neutrino sector. This means that in case (a) the dominant right-handed neutrino cannot be associated with the third family, whereas in case (b) it may be.

dilution suppression $d \lesssim 0.1$, implies from Eq.22 $Y_B \lesssim 10^{-10}$ which is just about acceptable.

We shall later present specific examples with detailed numerical results which support the conclusion that leptogenesis prefers case (b) where the dominant right-handed neutrino is the heaviest one, at least according to the standard hot big bang picture, ignoring effects of inflation.

4 Numerical Approach to $U(1)$ Family Symmetry Models

Our numerical results are based on the SRHND models [9],[10], with a $U(1)$ family symmetry. The idea of such a symmetry is that the three families of leptons are assigned different $U(1)$ charges, and these different charges then control the degree of suppression of the operators responsible for the Yukawa couplings, leading to Yukawa matrices with a hierarchy of entries, and approximate “texture” zeroes [13]. As usual it is assumed that the $U(1)$ is slightly broken by the VEVs of some fields $\theta, \bar{\theta}$ which are singlets under the standard model gauge group, but which have vector-like charges ± 1 under the $U(1)$ flavour symmetry. The $U(1)$ breaking scale is set by $\langle \theta \rangle = \langle \bar{\theta} \rangle$. Additional exotic vector matter with mass M_V allows an expansion parameter λ to be generated by a Froggatt-Nielsen mechanism [13],

$$\frac{\langle \theta \rangle}{M_V} = \frac{\langle \bar{\theta} \rangle}{M_V} = \lambda \approx 0.22 \quad (58)$$

where the numerical value of λ is motivated by the size of the Cabibbo angle. Small Yukawa couplings are generated effectively from higher dimension non-renormalisable operators corresponding to insertions of θ and $\bar{\theta}$ fields and hence to powers of the expansion parameter in Eq.58. The number of powers of the expansion parameter is controlled by the $U(1)$ charge of the particular operator. The lepton doublets, neutrino singlets, Higgs doublet and Higgs singlet relevant to the construction of neutrino mass matrices are assigned $U(1)$ charges $l_i, n_p, h_u = 0$ and σ . From this starting point one may then generate the neutrino Yukawa matrices as in [9]. The neutrino Dirac Yukawa

matrix is

$$\tilde{Y}^\nu = \begin{pmatrix} a_{11}\lambda^{|l_1+n_1|} & a_{12}\lambda^{|l_1+n_2|} & a_{13}\lambda^{|l_1+n_3|} \\ a_{21}\lambda^{|l_2+n_1|} & a_{22}\lambda^{|l_2+n_2|} & a_{23}\lambda^{|l_2+n_3|} \\ a_{31}\lambda^{|l_3+n_1|} & a_{32}\lambda^{|l_3+n_2|} & a_{33}\lambda^{|l_3+n_3|} \end{pmatrix} \quad (59)$$

where Eq.59 may be identified with Eq.35. The heavy Majorana matrix is

$$\tilde{Y}_{RR} = \begin{pmatrix} A_{11}\bar{\lambda}^{|2n_1+\sigma|} & A_{12}\bar{\lambda}^{|n_1+n_2+\sigma|} & A_{13}\bar{\lambda}^{|n_1+n_3+\sigma|} \\ A_{12}\bar{\lambda}^{|n_2+n_1+\sigma|} & A_{22}\bar{\lambda}^{|2n_2+\sigma|} & A_{23}\bar{\lambda}^{|n_2+n_3+\sigma|} \\ A_{13}\bar{\lambda}^{|n_3+n_1+\sigma|} & A_{23}\bar{\lambda}^{|n_3+n_2+\sigma|} & A_{33}\bar{\lambda}^{|2n_3+\sigma|} \end{pmatrix} \quad (60)$$

where A_{ij} and a_{ij} are undetermined coefficients, and $\bar{\lambda}$ is an independent expansion parameter relevant for the right-handed neutrino sector.⁵

The neutrino Yukawa matrices are generated in a particular basis defined by the $U(1)$ family symmetry. This corresponds to the starting basis defined by tildes in section 2, and numerically we follow the procedure to go to the diagonal right-handed neutrino basis, as outlined there. Note that we assume as an approximation that the charged lepton matrix is diagonal with positive eigenvalues in the starting basis. In practice this may be approximately achieved by a suitable choice of right-handed lepton $U(1)$ family charges, as discussed elsewhere [9],[10].

In our numerical analysis we take account of the fact that the theory does not determine the complex coefficients A_{ij} and a_{ij} which one has to choose in some range. This is not a special feature of the SRHND models, which we are focussing on in this paper, but a limitation of texture models based on a $U(1)$ family symmetry. Usually one simply assumes that the unknown coefficients are of order $\mathcal{O}(1)$ and, therefore, the structure in the Yukawa matrices is given by the expansion parameter rather than the coefficients. Our approach to this problem is to scan over the unknown coefficients randomly and to construct distributions for the various observables of interest. This way we are able to determine distributions for masses and mixings of a given model. Given the statistical nature of our approach, one question comes immediately to mind: What is the correct range of values one should choose for the coefficients? Lacking any theoretical background we have chosen for the coefficients the interval

⁵We are grateful to G.Ross for emphasising that the right-handed neutrino sector is controlled by an independent expansion parameter.

$$a_{ij}, A_{ij} \Rightarrow [\sqrt{\lambda}, 1/\sqrt{\lambda}] \times e^{i\phi_{ij}}, \quad \phi_{ij} \Rightarrow [0, 2\pi] \quad (61)$$

It should be noted, that this choice is *the minimum requirement for texture models to be sensible*, simply because any larger variation in the coefficients would destroy the texture one originally assumed to be the dominant feature of the mass matrices of interest.

A word of caution might be in order. Obviously the distributions which we calculate depend on our choice for a_{ij}, A_{ij} . Lacking further theoretical support for our choice, we can not evaluate the success of a given model in terms of confidence intervals. Instead our method is more minimalistic. We will consider a model to be a “good” model, if the main body of the distribution in a given observable coincides with or is close to the experimentally preferred value. Clearly, a model which fails even our simplistic test will fail even more badly under a more sophisticated numerical analysis. We would like to stress, however, that although the width of the peaks and the detailed shape of the distributions change under a change of the range of the coefficients, the *position of the peaks* remains nearly invariant.

In order to be able to compute the expectations for the leptogenesis “observable” ϵ_1 in the different models, our current computation goes beyond the one we discussed in a previous paper [24] in allowing the coefficients a_{ij}, A_{ij} to be complex. Since we do not have a theory of phases, we decided to choose the ϕ_{ij} in the full interval $[0, 2\pi]$. In other words, since we do not know about any mechanism suppressing phases effectively in the Yukawa couplings, we simply expect that all phases should be large.

So, our numerical procedure may be summarised as follows. First select a particular flavour model defined by a choice of $U(1)$ charges. Second select randomly a set of complex coefficients a_{ij} and A_{ij} . Third diagonalise the right-handed neutrino mass matrix to yield positive eigenvalues, and express the Dirac Yukawa matrix in this basis, as discussed in section 2.1. Fourth calculate the see-saw matrix m_{LL} and hence the physical neutrino masses and the MNS angles and three phases as discussed in section 2.2. Fifth calculate the leptogenesis parameters ϵ_1 and Y_B as discussed in section 2.3. Then the whole procedure is repeated for a different set of randomly chosen complex coefficients a_{ij} and A_{ij} , and the results are binned to build up distributions of the observable quantities. In the figures we show in the following we use random sets of 10^8 matrices for each of the distributions shown. Finally a

different model is selected corresponding to a different set of $U(1)$ charges and the whole procedure is repeated for the new model. We disregard the effect of renormalisation group radiative corrections in going from high energy to low energy, which has been demonstrated to be of the order of a few per cent for SRHND models [11]

5 Leptogenesis Decoupling

In this section we will discuss leptogenesis *decoupling*, namely, the fact that the leptogenesis observable ϵ_1 can take any value independent of the low energy observables, i.e. masses and mixings. Unfortunately this means that measurements of the solar angle or the MNS phase for example does not tell us anything about leptogenesis. On the other hand the results in this section also demonstrate another aspect of leptogenesis, namely that it can be used to resolve the ambiguity between different models which all lead to very similar predictions for low energy neutrino observables. In this way leptogenesis provides information about the high energy theory which would be impossible to determine by the measurement of low energy observables alone.

We will defer the discussion of Y_B until the next section and concentrate here only on the calculation of ϵ_1 , since the conversion of the CP asymmetry parameter to Y_B depends highly on the assumed thermal history of the universe, whereas the calculation of ϵ_1 is theoretically clean.

In Table 1 we give four examples of models based on different choices of flavour charges. For simplicity, we start by assuming that the expansion parameter in the right-handed neutrino sector is equal to the Wolfenstein parameter $\bar{\lambda} = \lambda$, as was assumed in [10]. Model FC1 was discussed analytically in [10], where it is seen that it yields a heavy Majorana matrix with an off-diagonal structure in the $U(1)$ charge basis. It satisfies the SRHND conditions, and has $a \sim b, c$ and so leads to the LMA solution. FC2 also has an off-diagonal heavy Majorana matrix, but has $a \ll b, c$ and so leads to the SMA solution.⁶ FC3 is also taken from [10], and is an example of a model with an approximately diagonal heavy Majorana matrix in the $U(1)$ charge basis. Using the analytic results in [10] we find the approxi-

⁶The latest data from the SNO collaboration [5] rather strongly disfavours the SMA solution [7].

| Models | l_1 | l_2 | l_3 | n_1 | n_2 | n_3 | σ | θ_{23} | θ_{13} | θ_{12} | R |
|--------|-------|-------|-------|---------------|----------------|----------------|----------|---------------|---------------|---------------|-------------|
| FC1 | -2 | 0 | 0 | -2 | 1 | 0 | 0 | 1 | λ^2 | 1 | λ^4 |
| FC2 | -3 | -1 | -1 | -3 | 0 | -1 | 3 | 1 | λ^2 | λ^2 | λ^4 |
| FC3 | -1 | 1 | 1 | $\frac{1}{2}$ | 0 | $-\frac{1}{2}$ | -1 | 1 | λ | 1 | λ^4 |
| FC4 | -1 | 1 | 1 | $\frac{1}{2}$ | $-\frac{1}{2}$ | $-\frac{1}{2}$ | -1 | 1 | λ | - | - |

Table 1: Flavour charges (FC) for four models, as discussed in the text, and approximate expectations for θ_{23} , θ_{13} , θ_{12} and R for the four different models.

mate expectations for the experimentally accessible quantities (θ_{23} , θ_{13} , θ_{12} and $R \equiv |\Delta m_{21}^2|/|\Delta m_{32}^2|$) where $\Delta m_{ij}^2 \equiv m_i^2 - m_j^2$ as given in Table 1. Thus FC1 is suitable for the LMA solution, FC2 for the SMA solution, FC3 for the LMA but with a larger CHOOZ angle than FC1, and FC4 is a model without SRHND which is consequently expected to give a larger value of R than models FC1-FC3 which all have SRHND. ⁷

Figure 1 shows the distributions for the solar ($s_\odot \equiv 4 \sin^2 \theta_{12} (1 - \sin^2 \theta_{12}^2)$), atmospheric ($s_{Atm} \equiv 4 \sin^2 \theta_{23} (1 - \sin^2 \theta_{23}^2)$) and CHOOZ ($s_C \equiv 4 \sin^2 \theta_{13} (1 - \sin^2 \theta_{13}^2)$) angles as well as for $R \equiv |\Delta m_{21}^2|/|\Delta m_{32}^2|$ for the four models given in table 1. As discussed above, the detailed shape of the distributions is different to the one we calculated previously [24] using *real* coefficients. The positions of the peaks of the various distributions, however, did not change allowing for complex phases.

Figure 4 shows the distributions in the leptogenesis observable ϵ for the models FC1-FC4. From the figures one might be tempted to think, that different low energy observables lead to different values of ϵ_1 and so might be distinguished. This is not true, and we now show that any of the models can be modified to give any desired value of ϵ_1 , while keeping the low energy observables approximately unchanged.

Let us consider as an example the model FC3 discussed above, which

⁷As a side remark we mention that for neutrinoless double beta decay, in flavour models which make use of the seesaw mechanism, one never expects that the effective Majorana neutrino mass ($\langle m_\nu \rangle = (m_{LL})_{11}$) measured in double beta decay is exactly zero. However, these models produce a hierarchical spectrum of left-handed neutrinos and thus one expects $\langle m_\nu \rangle$ to be small. In the models we have studied in this paper, one typically gets $\langle m_\nu \rangle \sim 10^{-3} eV$, albeit depending on the model and with a rather larger uncertainty.

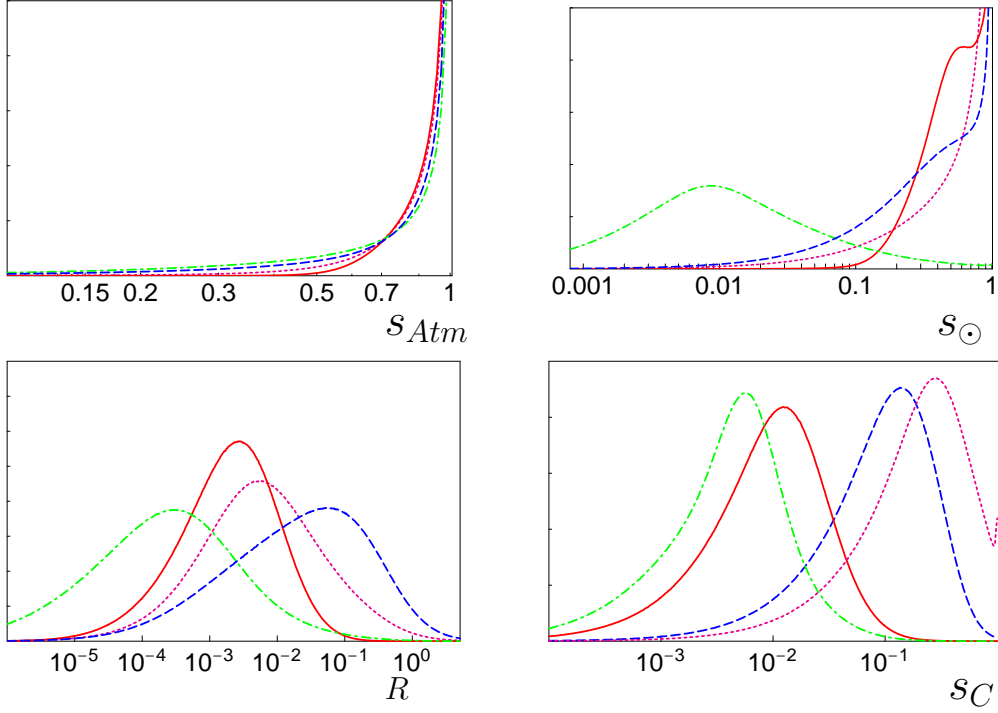


Figure 3: Theoretical distributions for the predictions of neutrino mass and mixing parameters for four selected see-saw models: FC1 (full), FC2 (dot-dashes), FC3 (thick dots), FC4 (dashes). Matrix coefficients are randomly chosen in the interval $[\sqrt{2\lambda}, 1/\sqrt{2\lambda}] \times e^{i\phi}$, with $\phi \Rightarrow [0, 2\pi]$. The vertical axis in each panel (deliberately not labelled) represents the *logarithmically binned* distributions with correct relative normalisation for each model, with heights plotted on a linear scale in arbitrary units.

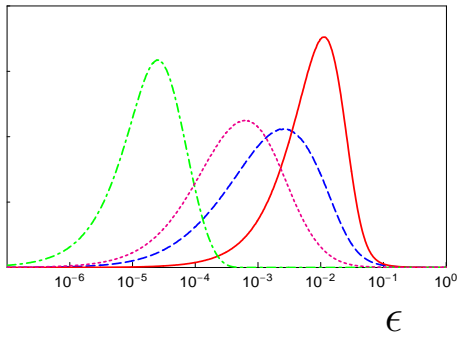


Figure 4: Plots of ϵ for the four different models of table 1. Plot style for different models follows fig. 3

predicts the LMA solution and a relatively large CHOOZ angle. Model FC3 gives (neglecting the coefficients and assuming $\bar{\lambda} = \lambda$) the following Dirac and Majorana mass matrices:

$$Y_\nu^{FC3} = \begin{pmatrix} \lambda^{1/2} & \lambda & \lambda^{3/2} \\ \lambda^{3/2} & \lambda & \lambda^{1/2} \\ \lambda^{3/2} & \lambda & \lambda^{1/2} \end{pmatrix} \quad (62)$$

$$Y_{RR}^{FC3} = \begin{pmatrix} 1 & \lambda^{1/2} & \lambda \\ \cdot & \lambda & \lambda^{3/2} \\ \cdot & \cdot & \lambda^2 \end{pmatrix} \quad (63)$$

which after see-sawing give the following leading order structure for m_{LL} :

$$m_{LL}^{FC3} \sim \begin{pmatrix} \lambda & 1 & 1 \\ 1 & \lambda^{-1} & \lambda^{-1} \\ 1 & \lambda^{-1} & \lambda^{-1} \end{pmatrix} + \mathcal{O} \left(\begin{pmatrix} \lambda & \lambda & \lambda \\ \lambda & \lambda & \lambda \\ \lambda & \lambda & \lambda \end{pmatrix} \right). \quad (64)$$

Note, that FC3 has a right-handed neutrino mass matrix which is diagonal to leading order and it is the lightest (third) right-handed neutrino which gives the dominant contribution to m_{LL} . The estimate for the asymmetry parameter is given in Eq.54, where it is clear that $e \sim \lambda^{1/2}$. In order to change ϵ_1 we must reduce e . This may be achieved by adjusting the l_i charges in such a way that the Dirac neutrino matrix just gets multiplied by an overall scaling factor compared to eq. 62, while the heavy Majorana Yukawa matrix remains unchanged. The rescaling of the Dirac Yukawa matrix implies that the coupling e is made smaller, and hence the scale of right-handed neutrino masses must be reduced in order to maintain the same value of m_3 . This will lead to a different value of ϵ_1 without changing the other low energy observables at all.

This qualitative conclusion is supported by our numerical results. In table 2 we give sets of charges for variants of the model FC3 of table 1, which lead to a simple rescaling of Y_ν ,

$$Y_\nu^{FC3(a,b,c,d,e)} = (\lambda^{(1,2,3,4,5)}) Y_\nu^{FC3} \quad (65)$$

and hence the scale of right-handed neutrino masses as shown in fig 5.

All of these models were constructed to preserve the low-energy phenomenology, and in fact we have checked that they lead to identical predictions for s_{Atm} , s_\odot , s_C and R as FC3. Figure 5 shows the resulting values

| Models | l_1 | l_2 | l_3 | n_1 | n_2 | n_3 | σ |
|--------|-------|-------|-------|---------------|-------|----------------|----------|
| FC3a | -2 | 2 | 2 | $\frac{1}{2}$ | 0 | $-\frac{1}{2}$ | -1 |
| FC3b | -3 | 3 | 3 | $\frac{1}{2}$ | 0 | $-\frac{1}{2}$ | -1 |
| FC3c | -4 | 4 | 4 | $\frac{1}{2}$ | 0 | $-\frac{1}{2}$ | -1 |
| FC3d | -5 | 5 | 5 | $\frac{1}{2}$ | 0 | $-\frac{1}{2}$ | -1 |
| FC3e | -6 | 6 | 6 | $\frac{1}{2}$ | 0 | $-\frac{1}{2}$ | -1 |

Table 2: “Variants” of the flavour model FC3 of table 1. All of these models give exactly the same distributions for the low energy neutrino observables. They differ, however, in their predicted values for the leptogenesis observable ϵ .

of M_1 and ϵ . Note that the lightest right-handed neutrino mass for FC3a, FC3b and FC3c in Fig.5 is above the reheat temperature allowed by the gravitino constraint [15]. This figure explicitly demonstrates that it is possible to completely decouple the predictions for leptogenesis from low energy observables.

How well do the analytic estimates for ϵ discussed previously agree with the numerical results? In terms of our small expansion parameter $\lambda \simeq 0.22$ and inserting the flavour charges for the models FC3 (FC3a, FC3b, FC3c, FC3d and FC3e) into eq. 52 one finds:

$$\epsilon_1^{(a)} \simeq \frac{3}{32\pi} \lambda^3 (\lambda^5, \lambda^7, \lambda^9, \lambda^{11}, \lambda^{13}) \quad (66)$$

numerically 3×10^{-4} (2×10^{-5} , 7×10^{-7} , 4×10^{-8} , 2×10^{-9} and 8×10^{-11}) which coincides approximately with the peaks of the distributions in ϵ shown in fig. 5. Recall that model FC3 predicts a right-handed neutrino mass matrix with the dominant neutrino being the lightest one (case a, discussed in section 3.2).

Model FC3 produces predictions for low-energy neutrino phenomenology

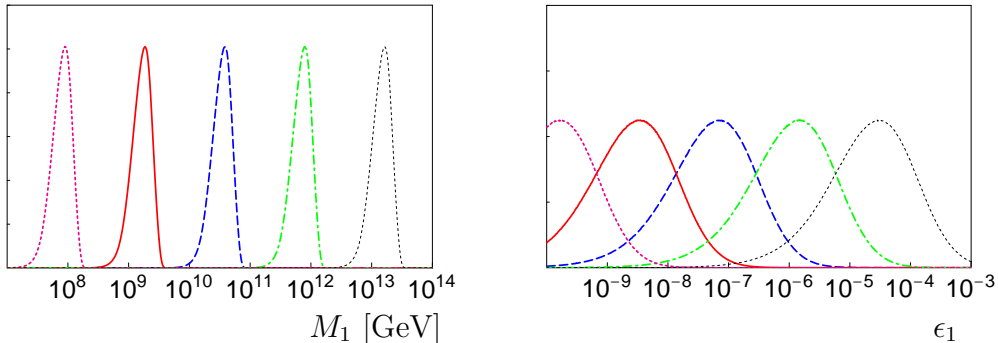


Figure 5: Plots of the mass of the lightest right-handed neutrino M_1 (left) and ϵ_1 (right) for the five different models of table 2. From right to left: FC3a-FC3e.

consistent with the large angle MSW solution of the solar neutrino problem. It is interesting to ask whether this solution is the only one for which one can decouple ϵ_1 from the low-energy observables.

In order to investigate this problem we have constructed variants of FC2, predicting a small angle MSW solution to the solar neutrino problem. The corresponding charges are given in Table. 3. All models in this table produce exactly the same distributions in R and s_{Atm} as model FC2, but lead to different predictions for s_\odot , s_C and ϵ_1 as is demonstrated in Fig. 6. Note that we have multiplied the distributions for FC2a and FC2b by a factor of 1.1, since otherwise the curves would completely overlap in some of the variables.

As can be seen from Fig. 6 models FC2 and FC2a give the same predictions for s_\odot and s_C , but differ in their predictions for ϵ_1 . FC2b and FC2c, on the other hand, give expectations for s_\odot and s_C which are smaller than the one for FC2 by about 1.5 orders of magnitude. Nevertheless, FC2b yields values of ϵ which are very similar to those of FC2. Also FC2c and FC2a have very similar expectations for leptogenesis while differing in s_\odot and s_C .

It is obviously easy to find models differing in their predictions for leptogenesis and at the same time being consistent with SMA MSW. Moreover,

| Models | l_1 | l_2 | l_3 | n_1 | n_2 | n_3 | σ |
|--------|-------|-------|-------|-------|-------|-------|----------|
| FC2 | -3 | -1 | -1 | -3 | 0 | -1 | 3 |
| FC2a | -4 | -2 | -2 | -3 | 0 | -1 | 3 |
| FC2b | -4 | -1 | -1 | -3 | 0 | -1 | 3 |
| FC2c | -5 | -2 | -2 | -3 | 0 | -1 | 3 |

Table 3: “Variants” of the flavour model FC2 of table 1. FC2 and FC2a give the same distributions for the low energy observables, with an expectation for the solar and CHOOZ angle of order λ^2 , FC2b and FC2c, on the other hand, lead to an expectation for solar and CHOOZ angle of order λ^4 . See fig. 6

neither the size of the solar nor the size of the CHOOZ angles tell us anything about whether leptogenesis is possible or not.

Finally we have investigated the question whether a special value of R determines ϵ_1 . All the models discussed so far prefer values of $R > 10^{-4}$. The following assignment of charges defines a model (FC5), which prefers larger hierarchies, see fig. 7,

$$(l_1, l_2, l_3, n_1, n_2, n_3, \sigma) = (3, -3, -3, 0, -1/2, 1, 1), \quad (67)$$

while still keeping the atmospheric and solar angles large (and $s_C \ll 1$). FC5 therefore is consistent with the LOW solution of the solar neutrino problem. Nevertheless, as fig. 7 demonstrates FC5 leads to a very similar expectation for ϵ as the model FC3b discussed above, which prefers R in the range $R \sim 10^{-3} - 10^{-2}$.

Obviously, any value of R can produce approximately the same order-of-magnitude values of ϵ_1 .

As a summary it can be stated that there is a decoupling between low energy neutrino observables and leptogenesis. We have demonstrated this point by constructing a number of different flavour models, which give the same predictions for neutrino masses and mixings while differing by huge factors in their expectations for leptogenesis.

On the other hand we have seen that leptogenesis is in principle able to resolve the ambiguity between different models which would lead to the same

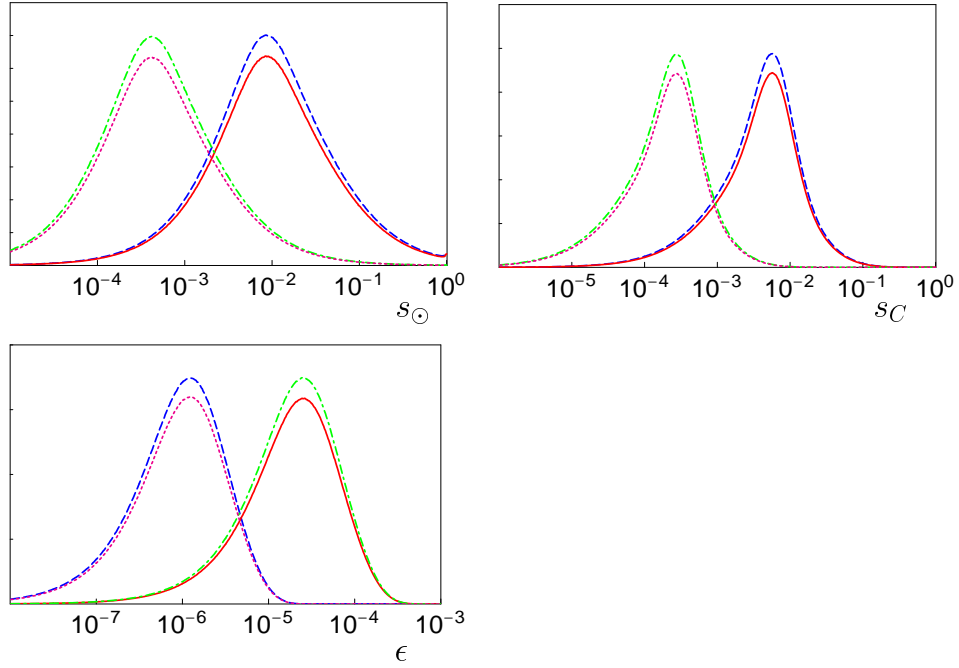


Figure 6: Plots of s_{\odot} (top left), s_C (top right), ϵ (bottom left) and Y_B (bottom right) for the four different models of table 3. The full line is FC2, the dashed line FC2a, the dotted line FC2b and the dash-dotted line FC2c. Note, that the distributions for FC2a and FC2b have been multiplied by a factor of 1.1, see text.

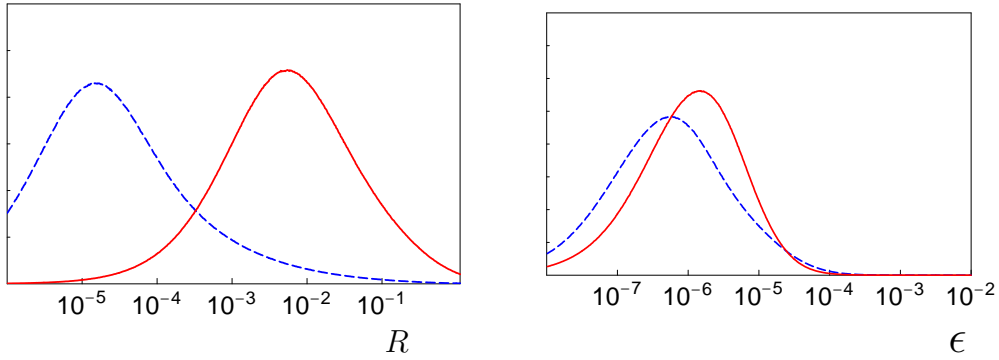


Figure 7: Plots of R (to the left) and ϵ (to the right) for the 2 different models FC3b (full line) and FC5 (dashed line).

low energy neutrino observables, and which otherwise would be indistinguishable. Therefore leptogenesis is able to provide information about the high energy theory which could not be obtained by low energy measurements.

6 From ϵ_1 to Y_B when the dominant right-handed neutrino is the lightest

While the calculation of ϵ_1 is straightforward, once a particular model has been specified, the calculation of Y_B depends crucially on a number of assumptions made about the early universe. In the following calculation we will assume a standard hot big bang scenario in which the maximum temperature is higher than the largest right-handed neutrino mass we consider, such that the right-handed neutrinos can be thermally produced. This assumption is necessary if one wants to employ one of the parameterizations to the full solution of the Boltzman equations, see eqs 26-27 and 30-32, discussed in section 2.3.

Obviously the following discussion will not be valid, if the universe underwent a period of inflation with a rather low reheat temperature, as required by the gravitino problem.

Let us first discuss the different values for Y_B one obtains using either eqs 26-27 or our parameterization eqs 30-32. As an example we will concentrate on the variants of the model FC3, discussed in the last section.

Fig. 8 shows calculated values of Y_B using the two different approximations. Obviously for large values of M_1 the two different calculations differ by many orders of magnitude. Using the simplest approximation, eqs 26-27, it seems that larger values of M_1 lead to larger values of Y_B and that, in principle, one can get Y_B as large as one desires. One can trace back this scaling to eq. 52 in section 3.2 and to the fact that eqs 26-27 do not depend on the value of M_1 .

On the other hand, using eqs 30-32, which take into account the suppression of Y_B for large values of M_1 and \tilde{m}_1 one gets a completely different picture. For large values of M_1 , Y_B is suppressed to negligible values and going to smaller values of M_1 increases Y_B . Note, however, that for the smallest values of M_1 of the order of $\mathcal{O}(10^8)$ [GeV] Y_B stops growing and never reaches the experimentally preferred range of $Y_B \sim (0.5 - 1) \times 10^{-10}$.

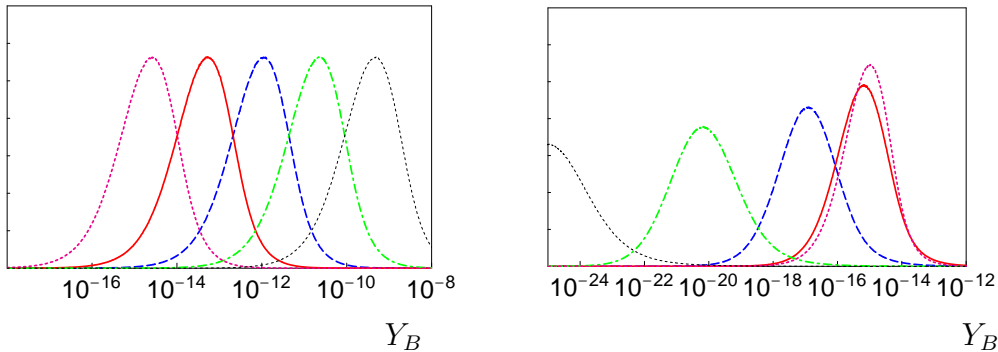


Figure 8: Plots of Y_B following eqs 26-27 (to the left) or according to eqs 30-32 (to the right) for the different variants of model FC3. Line style as in fig. 5.

All these variants of FC3 therefore fail the leptogenesis test.

Since the simple approximation, eqs 26-27 [21], employed similarly by a number of authors [20], fails to take into account any M_1 dependence of the dilution function its use would lead to the opposite conclusion. A careful treatment of d seems to be absolutely necessary for a reliable calculation of Y_B and we stress again that also our treatment is still only approximate.

In fig. 9 we plot Y_B as defined in eqs 22 and 33 with ϵ_1 estimated from eq. 54 and with d calculated by a) the simple approximation, defined in eqs 26-27 and b) our fit to the exact solution of the Boltzman equations [19], defined in eqs 30-32. For both calculations we fixed \tilde{m}_1 to $\tilde{m}_1 = 0.05$ eV. For small values of M_1 both approximations agree quite well, whereas for M_1 larger than $M_1 \sim 10^9$ GeV the expectations from the different approximations differ by many orders of magnitude.

One can understand the failure of the models FC3 to produce the correct value of Y_B on the basis of the discussion presented in section 2.3.⁸ From the analytic estimates presented in section 2.3 one finds that in models where the dominant right-handed neutrino is the lightest, \tilde{m}_1 depends on the same combination of Yukawas as the value of the heaviest neutrino mass, fixed by the atmospheric neutrino mass scale. Thus, for these models $\tilde{m}_1 \sim m_3 \sim 0.05$ eV. At such large values of \tilde{m}_1 , however, the dilution function d , see Fig. 1,

⁸For the analytic estimations of ϵ_1 and \tilde{m}_1 we assumed that the right-handed neutrino mass matrix is diagonal, which is approximately true for the variants of FC3.

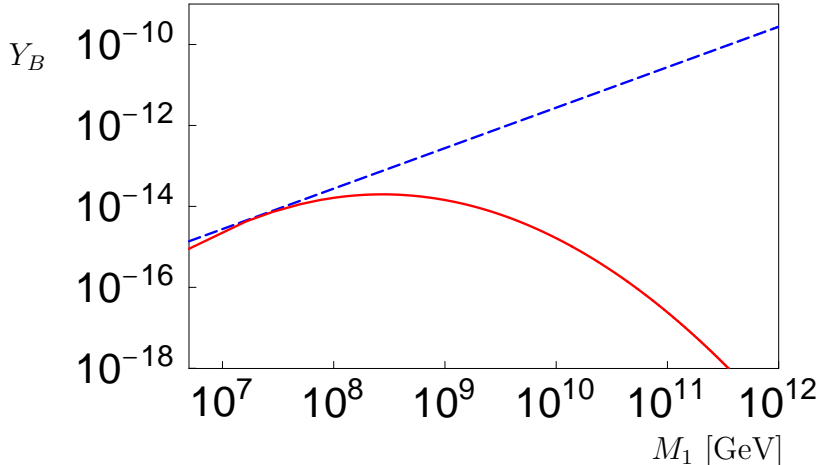


Figure 9: Plots of Y_B following eqs 26-27 (broken line) or according to eqs 30-32 (full line) assuming $\tilde{m}_1 = 0.05$ eV. For this plot we have assumed that ϵ_1 scales as given by eq. 54.

is heavily suppressed for values of M_1 larger than $M_1 \sim 10^8$ GeV. Thus, although larger values of M_1 lead to larger values of ϵ_1 , see eq. 54, the price one has to pay for such large masses in the dilution function always overcompensates and Y_B in these models can never be larger than $Y_B \sim 10^{-14}$ as is demonstrated in fig. 9.

Since all models where the dominant right-handed neutrino is the lightest share the feature $\tilde{m}_1 \sim m_3$, we conclude that upon use of eqs 30-32 they all fail the leptogenesis test. In the next section we will therefore study models in which the dominant right-handed neutrino is the heaviest.

7 Leptogenesis prefers models where the dominant right-handed neutrino is the heaviest

In the previous section we have seen that although leptogenesis is decoupled from the low energy neutrino observables, nevertheless leptogenesis is capable of resolving the ambiguities between classes of models which would otherwise lead to the same experimental predictions. As an example of the power of leptogenesis to give information about the high energy theory, in this

section we show that leptogenesis prefers models where the dominant right-handed neutrino is the heaviest one and discuss the implications of this for unified models. According to our analytic estimates we expect this class of models to yield a lightest right-handed neutrino mass which is lighter than in the previous case, and hence more acceptable from the point of view of the gravitino constraint. In addition these models may be more consistent with GUTs.

As a first example of a case (b) model we consider the charge vector

$$(l_1, l_2, l_3, n_1, n_2, n_3, \sigma) = (-3, 1, 1, 9, 1, -1, 2), \quad (68)$$

which defines a new model called FC9. The charges in Eq.68 lead to

$$Y_\nu^{FC9} \sim \begin{pmatrix} \lambda^6 & \lambda^2 & \lambda^4 \\ \lambda^{10} & \lambda^2 & 1 \\ \lambda^{10} & \lambda^2 & 1 \end{pmatrix} \quad (69)$$

and an approximately diagonal Majorana matrix

$$Y_{RR}^{FC9} \sim \begin{pmatrix} \bar{\lambda}^{20} & \bar{\lambda}^{12} & \bar{\lambda}^{10} \\ \bar{\lambda}^{12} & \bar{\lambda}^4 & \bar{\lambda}^2 \\ \bar{\lambda}^{10} & \bar{\lambda}^2 & 1 \end{pmatrix} \quad (70)$$

Now if we take $\bar{\lambda} = \sqrt{\lambda}$, this leads to the contributions from the heaviest (dominant), intermediate, and lightest right-handed neutrino, respectively, to the effective Majorana matrix of the order of,

$$m_{LL}^{FC9} \sim \begin{pmatrix} \lambda^8 & \lambda^4 & \lambda^4 \\ \lambda^4 & 1 & 1 \\ \lambda^4 & 1 & 1 \end{pmatrix} + \mathcal{O} \begin{pmatrix} \lambda^2 & \lambda^2 & \lambda^2 \\ \lambda^2 & \lambda^2 & \lambda^2 \\ \lambda^2 & \lambda^2 & \lambda^2 \end{pmatrix} + \mathcal{O} \begin{pmatrix} \lambda^2 & \lambda^6 & \lambda^6 \\ \lambda^6 & \lambda^{10} & \lambda^{10} \\ \lambda^6 & \lambda^{10} & \lambda^{10} \end{pmatrix}. \quad (71)$$

By inspection we see that the model predicts $\theta_{12} \sim 1$, $\theta_{13} \sim \lambda^4$, and, from the order λ^2 accuracy of the SRHND condition, $R \sim \lambda^4$. It may therefore be suitable for one of the large mixing angle solar solutions, either LMA or LOW. Assuming $\bar{\lambda} = \sqrt{\lambda}$, the lightest right-handed neutrino mass is predicted to be $X' \sim \lambda^{10} Y$, or $X' \sim 3 \cdot 10^{-7} Y \sim 10^8$ GeV, which is rather small. In order to increase X' we need to increase $\bar{\lambda}$.

As seen from Fig. 10 one can adjust the hierarchy in the right-handed sector by a rather small change in $\bar{\lambda}$. Going from $\bar{\lambda} = \sqrt{\lambda} \simeq 0.47$ to $\bar{\lambda} = 0.55$

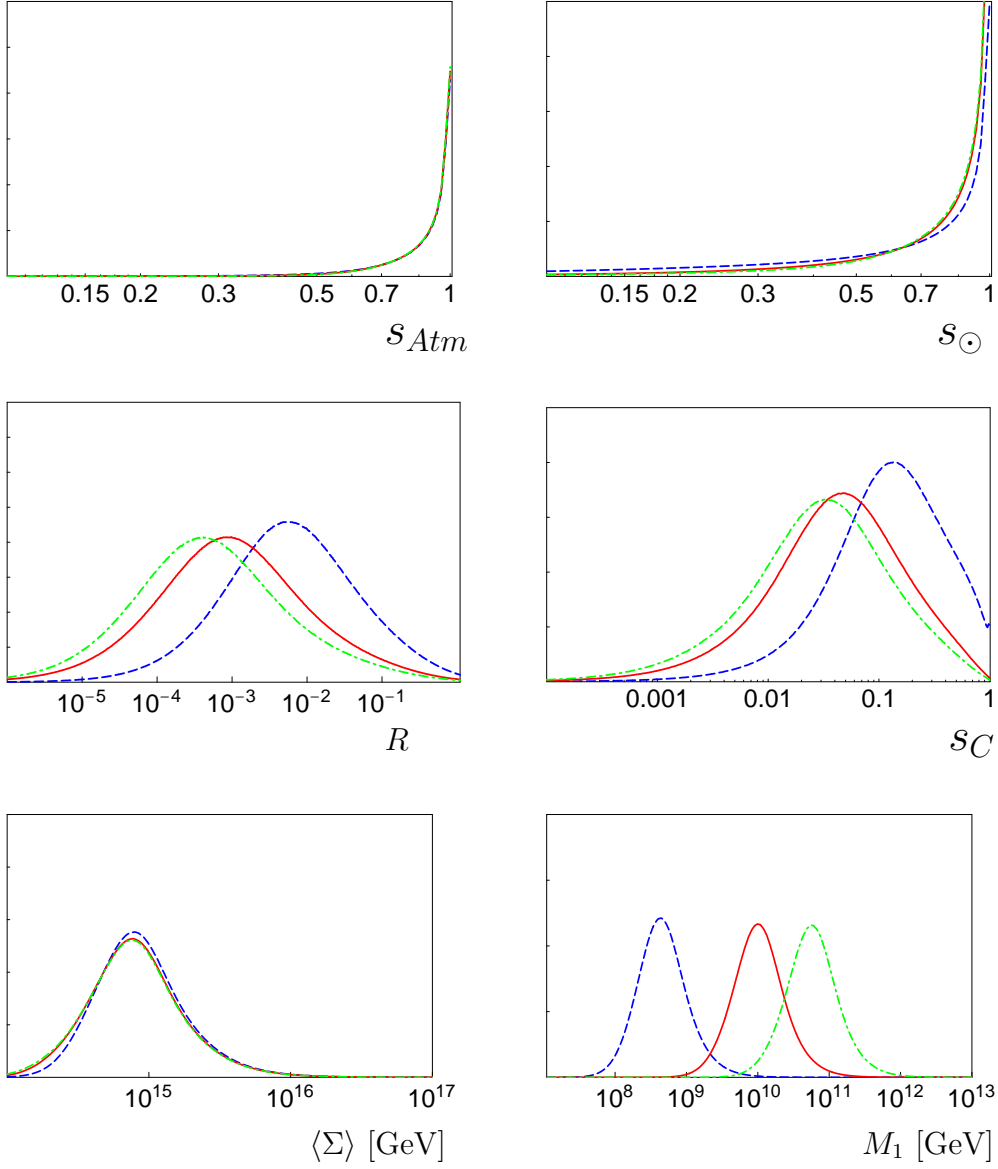


Figure 10: Plots of (from top left to bottom right: s_{Atm} , s_{\odot} , R , s_C , $\langle \Sigma \rangle$ and M_1 [GeV] for the model defined in eq. 68. Dashed line: $\bar{\lambda} = \sqrt{\lambda}$, full line: $\bar{\lambda} = 0.55$, dash-dotted: $\bar{\lambda} = 0.60$.

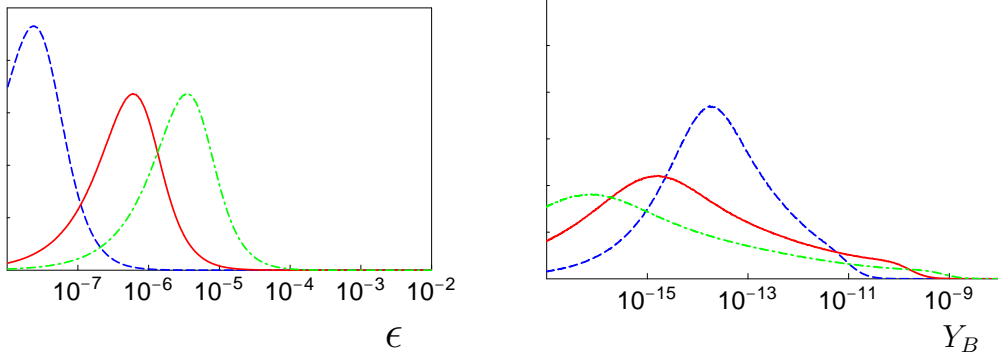


Figure 11: Plots of ϵ (to the left) and Y_B (to the right) for the model defined in eq. 68. Line styles are as in fig. 10.

(0.60) changes M_1 from $M_1 \sim (\text{few}) 10^8$ GeV to $M_1 \sim 10^{10}$ (10^{11}) GeV. This way it is possible to achieve larger values of ϵ and a value of Y_B marginally consistent with experimental data as shown in Fig. 11. Note, however, that the peaks in Y_B for this model are still too small and the models survive the leptogenesis test only in the tails of the distributions. Although in principle in models of this kind (case (b)) there is no association of the parameter $\tilde{m}_1^{(b)}$ in Eq.57 with a physical neutrino mass, in this case when we calculate $\tilde{m}_1^{(b)}$ we must first rotate to the basis in which the right-handed neutrino mass matrix is diagonal. This will lead to larger values of $\tilde{m}_1^{(b)} \sim 10^{-2} - 10^{-1}$ eV than would naively be estimated from Eq.69.

This change in $\bar{\lambda}$ also influences (although only rather weakly) the preferred values of R . As shown in Fig. 10 this model tends to prefer values of R consistent with the LOW solution of the solar neutrino problem. As mentioned previously, the LOW solution really only makes sense within the framework of SRHND because of the large hierarchies of neutrino masses which would otherwise appear rather unnatural.

One of the advantages of having the dominant right-handed neutrino as the heaviest is that leptogenesis may be achieved consistent with $e \sim 1$, which allows the third (dominant, and heaviest) right-handed neutrino to be associated with the third family in unified models. An example of such a model was recently presented in the framework of a string-inspired SUSY Pati-Salam (PS) model [25]. The model in [25] will not be repeated

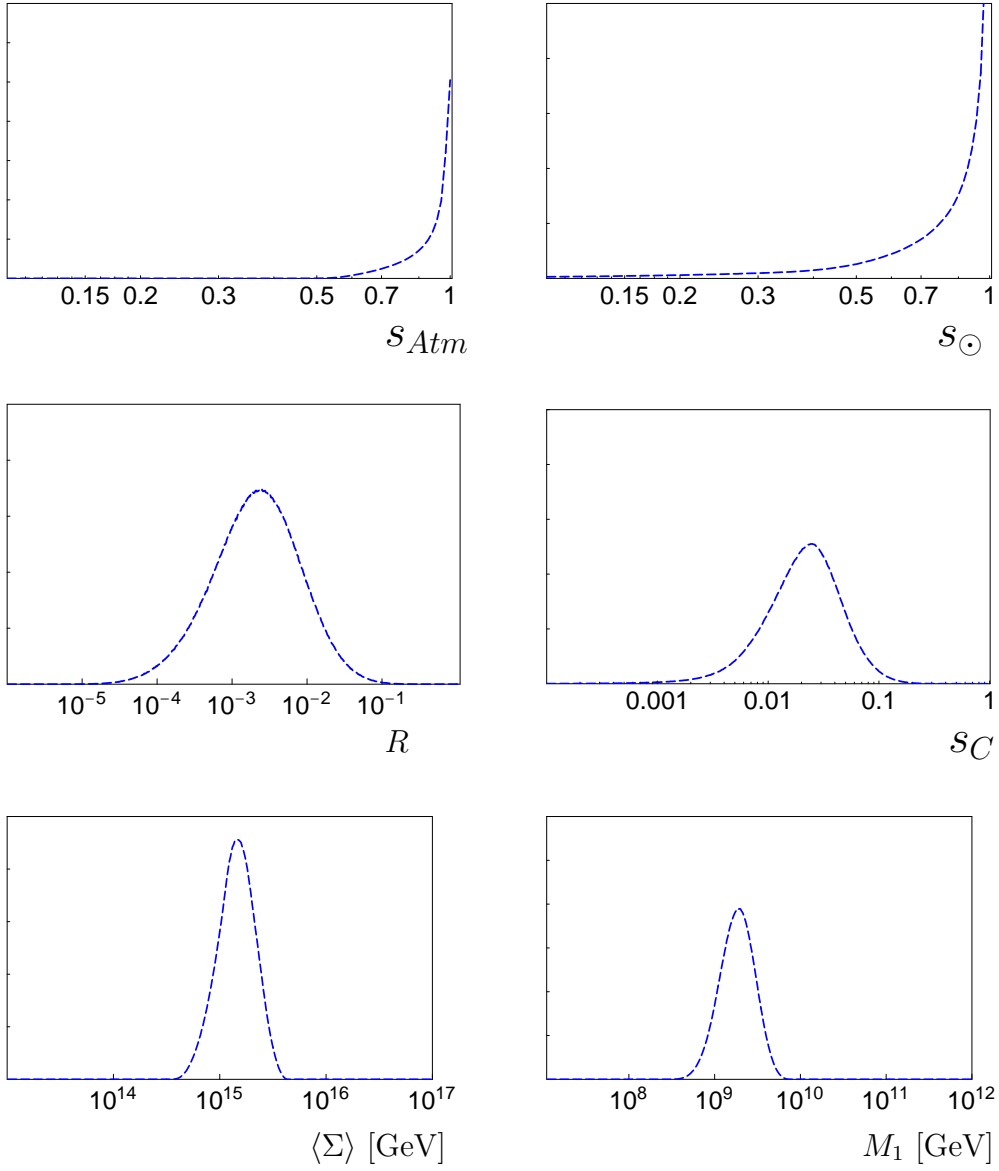


Figure 12: Plots of (from top left to bottom right: s_{Atm} , s_{\odot} , R , s_C , $\langle \Sigma \rangle$ and M_1 [GeV] for the Pati-Salam model discussed in eqs 72-73. Note that this model is consistent with the LA-MSW solution to the solar neutrino problem.

here, but we would emphasise that it was deduced from an analysis of the quark and lepton masses and mixing angles without any consideration of leptogenesis, and therefore we find it somewhat remarkable that it leads to a baryon asymmetry of the correct order of magnitude. The model in [25] leads to the following structure for the Yukawa and right-handed neutrino mass matrix:

$$Y_\nu^{PS} \sim \begin{pmatrix} \lambda^{7.5} & \lambda^{3.5} & \lambda^{1.5} \\ \lambda^{6.5} & \lambda^{3.5} & 1 \\ \lambda^{6.5} & \lambda^{3.5} & 1 \end{pmatrix} \quad (72)$$

$$M_{RR}^{PS} \sim \begin{pmatrix} \lambda^9 & \lambda^7 & \lambda^5 \\ \lambda^7 & \lambda^5 & \lambda^{3.5} \\ \lambda^5 & \lambda^{3.5} & 1 \end{pmatrix} \quad (73)$$

The effective light Majorana matrix then has contributions from the third, second and first right-handed neutrinos of:

$$m_{LL}^{PS} \sim \begin{pmatrix} \lambda^3 & \lambda^{1.5} & \lambda^{1.5} \\ \lambda^{1.5} & 1 & 1 \\ \lambda^{1.5} & 1 & 1 \end{pmatrix} + \mathcal{O} \begin{pmatrix} \lambda^2 & \lambda^2 & \lambda^2 \\ \lambda^2 & \lambda^2 & \lambda^2 \\ \lambda^2 & \lambda^2 & \lambda^2 \end{pmatrix} + \mathcal{O} \begin{pmatrix} \lambda^6 & \lambda^5 & \lambda^5 \\ \lambda^5 & \lambda^4 & \lambda^4 \\ \lambda^5 & \lambda^4 & \lambda^4 \end{pmatrix}. \quad (74)$$

From the analytic estimates in 3.1 we expect this model to be consistent with the LMA MSW solution. This is explicitly demonstrated in Fig. 12. From the analytic estimates in 3.2 we also expect this model to give successful leptogenesis, and this is demonstrated in Fig. 13. From the matrices given above and from the analytical estimates of eq. 53 one expects that $\epsilon_1 \sim 3/(16\pi) \times \lambda^9 \sim 7 \times 10^{-8}$, which within a factor of ~ 2 or so agrees with the numerical calculation of ϵ_1 in fig. 13. Note, that the resulting values of Y_B in fig. 13 are also consistent with the arguments in 3.2. In particular in such case (b) models where the dominant right-handed neutrino is the heaviest it is easier to avoid the gravitino constraint [15], although the values of M_1 are still a bit on the high side, as seen in fig. 12. As in the previous model, in the diagonal right-handed neutrino basis we obtain a larger value of $\tilde{m}_1^{(b)} \sim 10^{-2}$ eV than would naively be estimated from Eq.72.

Note that supersymmetric models of case (b) have the feature that there is an order unity Yukawa coupling in the 23 position of the Yukawa matrix which leads to a large off-diagonal entry in the slepton mass matrix. This

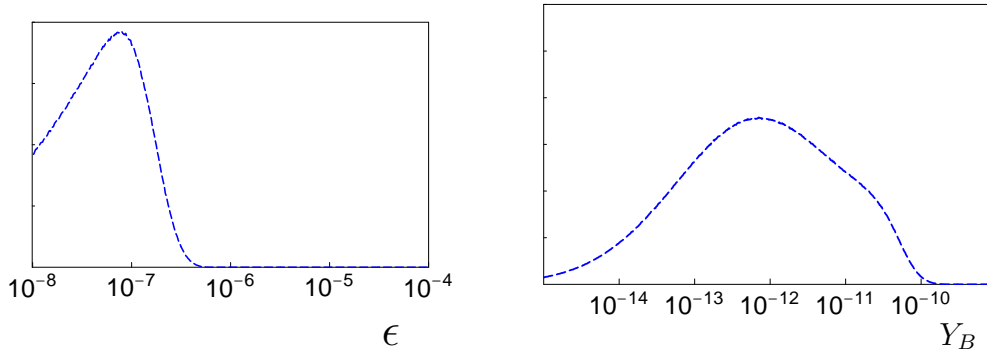


Figure 13: Plots of ϵ (to the left) and Y_B (to the right) for the Pati-Salam model of [25].

leads to the striking signature of the lepton flavour violating (LFV) process $\tau \rightarrow \mu\gamma$ close to the experimental upper limit, as first pointed out in [27]. In general LFV constraints provide an additional window into the see-saw matrices in supersymmetric models [27, 28].

8 Summary and Conclusions

This paper represents the first study of leptogenesis based on hierarchical models of neutrino masses in which SRHND is used to generate the neutrino mass hierarchy. Such models have been shown to accommodate the presently favoured large solar angle solutions such as LMA and LOW [10], and in the case of the LOW solution where the neutrino mass hierarchy is large it would seem that SRHND is almost inevitable. So we would argue that, far from this analysis being restricted to a particular small class of models, it is in fact quite generally applicable to large classes of models in which the neutrino mass hierarchy is generated in a natural way without any fine-tuning. Therefore the above results should be regarded as being quite generally applicable to see-saw models containing a neutrino mass hierarchy.

In presenting our analytic and numerical results we make a clear distinction between the theoretically clean asymmetry parameter ϵ_1 and the baryon

asymmetry Y_B , for which we present and use a fit based on a Boltzmann analysis. We have presented analytic expressions for both the MNS parameters, extending the previously presented analytic results [10] to the complex domain, and for leptogenesis asymmetry parameter ϵ_1 in the cases where the dominant right-handed neutrino is either the heaviest or the lightest. We have compared the analytic estimates to full numerical results for models based on $U(1)$ family symmetry, and have performed a numerical scan over the unknown coefficients, and have seen that the peaks of the distributions in ϵ_1 are in good agreement with the analytic results. Using the analytic and numerical approaches we then discussed leptogenesis decoupling and leptogenesis discrimination.

We have shown that quite generally there is a decoupling between the low energy neutrino observables and the leptogenesis predictions for ϵ_1 . Thus leptogenesis has nothing to tell us about which solar solution we would expect, and for example the LMA and the LOW solutions are equally acceptable, as indeed would have been the SMA solution were it not disfavoured by SNO and Super-Kamiokande. Furthermore the leptogenesis phase is independent of the measurable MNS phase, although the analytic estimates make it clear that since the two phases originate from the same Yukawa matrix, and even in some cases involve the phases of the same Yukawa couplings, the general expectation is that, barring cancellations, both sorts of phases should be of roughly the same order of magnitude.

In going from ϵ_1 to Y_B one needs to make some assumptions concerning the cosmological history of the universe. In this paper we have assumed a standard hot big bang universe, which is equivalent to assuming a very high reheat temperature after inflation which is larger than the right-handed neutrino masses. Within this standard cosmology the right-handed neutrinos are produced via their couplings to the thermal bath, yet they are required to decay out-of-equilibrium, leading to a rather narrow range of couplings \tilde{m}_1 of the lightest right-handed neutrino consistent with successful leptogenesis. For the calculation of Y_B a correct treatment of the Boltzmann equations describing the number evolution of the heavy right-handed neutrinos in the early universe is essential [19]. We therefore have devised an empirical fit formula and compared it to the exact results [19] as well as to the simpler approximation [20, 21]. Although for a small range in \tilde{m}_1 and small values of the lightest right-handed neutrino mass the simple approximation [20, 21] agrees reasonably with the exact result [19], for most parts of the param-

eter space it fails badly. Only if one takes into account the suppression of the dilution factor d for larger values of \tilde{m}_1 and M_1 , either by solving the Boltzman equations numerically or by the use of our approximate fit formula, does one find reliable results. Without taking this effect into account we would have wrongly concluded that Y_B can get as large as $Y_B \sim 10^{-5}$ in some models, whereas with our more refined treatment we find that Y_B is always $Y_B \leq 10^{-14}$, if the dominant right-handed neutrino is the lightest.

Based on the above analysis of Y_B we have shown that leptogenesis excludes a large class of models where the dominant right-handed neutrino is the lightest one. The power of leptogenesis to resolve ambiguities between models which would otherwise lead to the same neutrino observables provides a welcome constraint on high energy theories. We have shown that models where the dominant right-handed neutrino is the heaviest are marginally consistent with the gravitino constraint and have studied an explicit example of a unified model of this type. We find it encouraging that a model which was written down to describe the fermion mass spectrum [25], including the neutrino spectrum and the LMA MSW solution, should be precisely of this kind and gives successful leptogenesis, subject to the uncertainties of our estimates discussed in section 2.3.

Finally we should emphasise that our conclusions are based on the assumed cosmological history being the standard hot big bang with a high reheat temperature. One plausible alternative is to suppose that the reheat temperature is below 10^9 GeV, but that heavier right-handed (s)neutrinos can be produced in sufficient numbers by preheating at the end of inflation [29]. The preheating must efficiently produce right-handed (s)neutrinos without over-producing gravitinos, and this will depend on the precise details of the inflation model. A model of leptogenesis with a low reheat temperature, based on preheating of heavy right-handed sneutrinos, which does not suffer from the gravitino problem has been recently studied in detail in [26]. The same Pati-Salam model has also been studied in this context [26] and interestingly the results for Y_B are also consistent, within the large uncertainty, with the estimates given here, based on an entirely different cosmological history of the universe.

Acknowledgements

We thank M.Plümacher for various discussion on the numerical solution to the

Boltzman equations. S.K. is grateful to PPARC for the support of a Senior Fellowship.

References

- [1] M. Fukugita and T. Yanagida, Phys. Lett. **B174** (1986) 45.
- [2] M. A. Luty, Phys. Rev. **D45** (1992) 455.
- [3] G. t'Hooft, Phys. Rev. Lett. **37** (1976) 8; V. A. Kuzmin, V. A. Rubakov and M. E. Shaposhnikov, Phys. Lett. **B155** (1985) 36; J. Ambjrn, T. Askgaard, H. Porter and M. E. Shaposhnikov, Nucl. Phys. **B353** (1991) 346.
- [4] M. Gell-Mann, P. Ramond and R. Slansky in Sanibel Talk, CALT-68-709, Feb 1979, and in *Supergravity* (North Holland, Amsterdam 1979); T. Yanagida in *Proc. of the Workshop on Unified Theory and Baryon Number of the Universe*, KEK, Japan, 1979.
- [5] The SNO collaboration, nucl-ex/0106015
- [6] Super-Kamiokande Collaboration, S. Fukuda et al., hep-ex/0103033 and hep-ex/0103032; Super-Kamiokande collaboration, Phys. Lett. **B436** (1998) 33.;
- [7] J.N. Bahcall, M. C. Gonzalez-Garcia and Carlos Pena-Garay, hep-ph/0106258; G.L. Fogli, E. Lisi, D. Montanino and A. Palazzo, hep-ph/0106247.
- [8] M. Flanz, E. A. Paschos, U. Sarkar and J. Weiss, Phys. Lett. **B389** (1996) 693; A. Pilaftsis, Phys. Rev. **D56** (1997) 5431; W. Buchmüller and T. Yanagida, Phys. Lett. **B445** (1999) 399; J. Ellis, S. Lola and D. V. Nanopoulos, hep-ph/9902364; M. S. Berger and B. Brahmachari, hep-ph/990340; R. Barbieri, P. Creminelli, A. Strumia and N. Tetradis, hep-ph/9911315; H. Murayama, H. Suzuki and T. Yanagida, Phys. Rev. Lett. **70** (1993) 1912; B. A. Campbell, S. Davidson and K. A. Olive, Nucl Phys. **B399** (1993) 111; H. Murayama and T. Yanagida, Phys. Lett. **B322** (1994) 349; T. Moroi and H. Murayama, hep-ph/9908223;

- T. Asaka, K. Hamaguchi, M. Kawasaki and T. Yanagida, Phys. Rev. D **61** (2000) 083512 [hep-ph/9907559]; R. Jeannerot, Phys. Rev. Lett. **77** (1996) 3292 [hep-ph/9609442]; W. Buchmüller and T. Yanagida, Phys. Lett. **B302** (1993) 240; W. Buchmüller and M. Plümacher, Phys. Lett. **B431** (1998) 354; R.N. Mohapatra and X. Zhang, Phys. Rev. **D46** (1992) 5331
- [9] S. F. King, Phys. Lett. **B439** (1998) 350; S. F. King, Nucl. Phys. **B562** (1999) 57.
- [10] S. F. King, Nucl. Phys. **B576** (2000) 85.
- [11] S. F. King and N. N. Singh, Nucl. Phys. B **591** (2000) 3.
- [12] For a non-exhaustive list of recent reviews, see for example: G. Altarelli and F. Feruglio, Phys. Rep. **320** (1999) 295; R. N. Mohapatra, hep-ph/0008232; J.W.F. Valle, hep-ph/9911224; S.M. Bilenky, C. Giunti, W. Grimus, Prog.Part.Nucl.Phys. 43 (1999) 1-86; S.F. King, hep-ph/0105261.
- [13] C. D. Froggatt and H. B. Nilsen, Nucl. Phys. B147 (1979) 277; L. Ibanez and G.G. Ross, Phys. Lett. B332 (1994) 100; P. Binetruy and P. Ramond, Phys. Lett. B350 (1995) 49.
- [14] Z. Maki, M. Nakagawa and S. Sakata, Prog. Theo. Phys. **28** (1962) 247.
- [15] E. Holtmann, M. Kawasaki, K. Kohri and T. Moroi, Phys. Rev. D **60** (1999) 023506 [hep-ph/9805405], and references therein.
- [16] L. Covi, E. Roulet and F. Vissani, Phys. Lett. **B384** (1996) 169; L. Covi, E. Roulet and F. Vissani, Phys. Lett. **B424** (1998) 101.
- [17] For a review see W. Buchmüller and M. Plümacher, hep-ph/9904310; M. Plumacher, hep-ph/9807557.
- [18] W. Buchmüller and M. Plümacher, Phys. Lett. **B389** (1996) 73; M. Plümacher, Z. Phys. **C74** (1997) 549; M. Plümacher, Nucl. Phys. **B530** (1998) 207
- [19] W. Buchmüller and M. Plümacher, Int. J. Mod. Phys. **A15** (2000) 5047 [hep-ph/0007176]

- [20] E.W. Kolb and M.S. Turner, The early Universe (Addison-Wesley, 1990); A. Pilaftsis, Int. J. Mod. Phys. A14 (1999) 1811; M. Flanz and E.A. Paschos, Phys. Rev. **D58** (1998) 113009; D. Falcone and F. Tramontano, hep-ph/0101151.
- [21] H.B. Nielson and Y. Takanishi, hep-ph/0101307
- [22] J.A. Harvey and M.S. Turner, Phys. Rev. **D42** (1990) 3344; S.Y. Khlebnikov and S.E. Shaposhnikov, Nucl. Phys. **B308** (1998) 169
- [23] M. Apollonio *et al.*, Phys.Lett. **B466** (1999) 415.
- [24] M. Hirsch and S.F. King, hep-ph/0102103
- [25] S. F. King, M.Oliveira, Phys.Rev. **D63** (2001) 095004
- [26] M. Bastero-Gil and S.F. King, Phys. Rev. **D63** (2001) 123509, [hep-ph/0011385]
- [27] T. Blazek and S. F. King, hep-ph/0105005.
- [28] S. Lavignac, I. Masina and C. A. Savoy, hep-ph/0106245; S. Davidson and A. Ibarra, hep-ph/0104076; J. R. Ellis, M. E. Gomez, G. K. Leontaris, S. Lola and D. V. Nanopoulos, Eur. Phys. J. C **14** (2000) 319 [hep-ph/9911459]; F. Borzumati and A. Masiero, Phys. Rev. Lett. **57** (1986) 961.
- [29] G. F. Giudice, M. Peloso, A. Riotto and I. Tkachev, JHEP **9908** (1999) 014 [hep-ph/9905242].